

A New Look at Bounding Integrity Risk in the Presence of Time-Correlated Errors

Steven E. Langel, *The MITRE Corporation*

Mathieu Joerger, *The University of Arizona*

Samer M. Khanafseh and Boris S. Pervan, *Illinois Institute of Technology*

BIOGRAPHIES

Dr. Steven Langel is a senior member of the technical staff at The MITRE Corporation's National Security Engineering Center. He received his B.S. (2006) and Ph.D. (2014) in mechanical and aerospace engineering from the Illinois Institute of Technology. In his role as trusted advisor to the U.S. government, Dr. Langel designs advanced multi-sensor navigation systems, derives and analyzes fault detection algorithms, and studies fundamental behavior of faulted systems. Steven also continues to engage and perform research in high accuracy/high integrity navigation. Specifically, he is developing new algorithms that properly quantify and bound the effect of measurement error model uncertainty on navigation system integrity. He is an active member of the Institute of Navigation (ION).

Dr. Mathieu Joerger obtained a 'Diplôme d'Ingénieur' (2002) from the Ecole Nationale Supérieure des Arts et Industries de Strasbourg, in France, and an M.S. (2002) and Ph.D. (2009) in Mechanical and Aerospace Engineering from the Illinois Institute of Technology in Chicago. He is the 2009 recipient of the Institute of Navigation (ION)'s Bradford Parkinson award, and the 2014 recipient of the ION's Early Achievement Award. Dr. Joerger is currently assistant professor at the University of Arizona, working on multi-constellation Global Navigation Satellite Systems (GNSS) for safety-critical civilian aviation applications, on multi-sensor integration, fault detection, and exclusion for highly automated ground vehicle navigation, and on trajectory tracking risk evaluation for space debris.

Dr. Samer Khanafseh is currently a research assistant professor at Illinois Institute of Technology (IIT), Chicago. He received his M.S. and PhD degrees in Aerospace Engineering at IIT, in 2003 and 2008, respectively. Dr. Khanafseh has been involved in several aviation applications such as Autonomous Airborne Refueling (AAR) of unmanned air vehicles, autonomous shipboard landing for the UCAS and JPALS programs and Ground Based Augmentation System (GBAS). His research interests are focused on high accuracy and high integrity navigation algorithms for close proximity applications, cycle ambiguity resolution, high integrity applications, fault monitoring and robust estimation techniques. He was the recipient of the 2011 Institute of Navigation Early Achievement Award for his outstanding contributions to the integrity of carrier phase navigation systems.

Dr. Boris Pervan is a Professor of Mechanical and Aerospace Engineering at IIT, where he conducts research on advanced navigation systems. Prior to joining the faculty at IIT, he was a spacecraft mission analyst at Hughes Aircraft Company (now Boeing) and a postdoctoral research associate at Stanford University. Prof. Pervan received his B.S. from the University of Notre Dame, M.S. from the California Institute of Technology, and Ph.D. from Stanford University. He was the recipient of the IIT Sigma Xi Excellence in University Research Award, Ralph Barnett Mechanical and Aerospace Dept. Outstanding Teaching Award, Mechanical and Aerospace Dept. Excellence in Research Award, IIT University Excellence in Teaching Award, IEEE Aerospace and Electronic Systems Society M. Barry Carlton Award, RTCA William E. Jackson Award, Guggenheim Fellowship (Caltech), and the Albert J. Zahm Prize in Aeronautics (Notre Dame). He is an Associate Fellow of the AIAA, a Fellow of the Institute of Navigation (ION), and Editor-in-Chief of the ION Journal Navigation.

ABSTRACT

A new approach is developed to upper bound integrity risk for safety-critical GNSS applications when the autocorrelation functions of measurement and process noise are uncertain. The algorithm is recursive and significantly expands the applicable range of existing methods. In Kalman filtering, models must be specified for autocorrelated measurement and process noise. This paper assumes that the noise processes are the output of known linear systems driven by white noise. However, the system

parameters are only known to lie in specified intervals. Following the approach in [6], an augmented state model is first developed to propagate the estimate error covariance matrix when there is parameter uncertainty. It is shown that the error variance for a specified state is a polynomial in the unknown parameters whose order grows linearly with time. An exact upper bound on integrity risk is determined by maximizing the variance. Next, a recursive algorithm is derived to update the variance's Taylor series expansion. This enables an approximate bound to be established by maximizing a polynomial whose order is low and remains fixed over time. The Taylor remainder theorem is used to introduce conservatism and provide justification that the approximate bound is at least as large as the exact bound. For a one-dimensional navigation problem, we show that the number of series terms needed to obtain a tight upper bound on integrity risk is less than 10.

INTRODUCTION

Safety-critical GNSS applications must ensure that the probability of the estimate error exceeding predefined bounds is acceptably small. This probability is referred to as *integrity risk*. Stochastic measurement error models play a dominant role in determining the estimate error probability density function. These models always have some element of uncertainty and should be defined so that computed integrity risk always upper bounds the true risk. In the aviation community, the concept of cumulative distribution function (CDF) overbounding was established as a methodology to guarantee conservative assessments of integrity risk if the measurement noise is independent [1], [2]. For snapshot weighted least squares estimation using pseudorange measurements, this assumption can be justified. However, it is becoming more common to fuse GNSS with other sensors (e.g., an IMU) and perform state estimation using a Kalman filter. Autonomous vehicle navigation is one application where multiple sensors in addition to GNSS are used to estimate the vehicle's state. When measurement errors are correlated over time (not uncommon in practice), the independence assumption is no longer valid and CDF overbounding cannot be used to establish an integrity risk bound. Without a rigorous methodology, filter designers rely on intuition to establish bounds. For example, it seems reasonable to suspect that the estimate error variance will increase as measurement errors become more correlated because the measurements contain less information. Therefore, error models with maximum correlation should be used to design the Kalman filter. No analysis was done to verify the hypothesis, which turns out to be wrong (we'll see an example later). Over the past ten years, several research papers have emerged that seek to provide a mathematically sound approach to integrity risk bounding in the presence of correlated errors.

A theoretical approach was described in [3] and [4] for bounding the integrity risk of linear systems driven by correlated noise. If the input noise vectors can be linearly mapped from a spherically symmetric space, the authors showed how to transform a CDF overbound on any input noise component into an overbound on the state estimate error. In [5], the authors considered the case where measurement and process noise are Gaussian random processes whose autocorrelation functions (ACFs) are only known to lie between specified lower and upper bounds. The estimate error variance was expressed as a linear combination of all past and current ACF values and then maximized by setting the ACFs equal to their upper or lower bound based on the sign of the coefficient. References [3] – [5] provide batch solutions in the sense that they store the effect of all current and past input noise samples on the estimate error vector. This is not a limitation, but rather a consequence of not prescribing any structure on the input noise ACFs. The ability of these methods to provide a real-time integrity risk bound is limited to short-duration applications whose length is dependent on sensor sampling rates. To expand the range of applicability, structure must be imposed on the ACFs.

This paper assumes that the noise processes are the output of linear systems driven by white noise. However, the parameters defining the system are only known to lie in specified intervals. Numerous articles in the robust estimation literature derive linear estimators that achieve specific measures of optimality in the presence of uncertainty. These approaches will not be considered here for two reasons. First, they are often used to design filters off-line and involve computationally intensive algorithms to determine the estimator gain (e.g., semi-definite programming). Second, robust linear estimators tend to be overly conservative and provide bounds on the covariance matrix that are very sensitive to tuning parameters chosen based on engineering judgement or trial and error. In [6], the Kalman filter is defined using any set of admissible parameter values chosen by the filter designer. Although the Kalman filter is no longer optimal in this case, new estimate error equations can be derived that enable one to quantify the effect of model uncertainty on the estimate error covariance matrix. Intended as an off-line analysis tool, the Kalman filter is run repeatedly with different values of the true parameters to assess sensitivity. Reference [7] considers the specific case where measurement noise is first-order Gauss Markov with an unknown time constant. In addition to assuming the true parameters are unknown, the authors also allow the filter parameter values to vary. The minimum upper bound on integrity risk is defined as a mini-max optimization problem, whose solution is determined using a bank of Kalman filters.

An alternative approach to upper bound integrity risk is derived in this paper that represents a significant improvement over the methods in [6] and [7]. The paper is organized as follows. Section I introduces the problem, which is simplified to one measurement noise component and no process noise. The measurement noise is known to be a first order Gauss-Markov process with a transition parameter that is lower and upper bounded. The results obtained for the simplified problem extend naturally to the general case of multiple measurement and process noise components. Section II follows the approach in [6] to develop estimate error equations that conveniently express the covariance matrix in terms of the unknown parameter. It is shown that the error variance for a specified state is a polynomial in the unknown parameter whose order grows linearly with time. An exact upper bound on integrity risk is determined by maximizing the variance. A recursive algorithm is derived in Section III to update the error variance's Taylor series expansion. This enables an approximate bound to be established by maximizing a polynomial whose order is low and remains fixed over time. The Taylor remainder theorem is used to introduce conservatism and provide justification that the approximate bound is at least as large as the exact bound. The methods are applied to a one-dimensional GNSS navigation problem in Section IV, where it is shown that the number of terms needed to obtain a tight upper bound on integrity risk is low (less than 10). Concluding remarks and suggestions for future work are provided in Section V.

PROBLEM STATEMENT

This paper considers the simplified linear system

$$\begin{aligned}\mathbf{x}_{k+1} &= \mathbf{A}_k \mathbf{x}_k \\ z_k &= \mathbf{C}_k \mathbf{x}_k + v_k\end{aligned}\tag{1}$$

where \mathbf{x}_k is the state vector, z_k is the measurement and v_k is zero-mean Gaussian measurement noise. Suppose that $v_k = m_k + r_k$, such that r_k is zero-mean white Gaussian noise with variance σ_r^2 and m_k is a first order Gauss-Markov process with transition parameter a and variance σ_m^2 . The first order Gauss-Markov process evolves according to [6]

$$m_{k+1} = am_k + \sigma_m(1 - a^2)^{1/2}w_k\tag{2}$$

with $w_k \sim N(0,1)$. The variances σ_r^2 and σ_m^2 are known, but a is only known to lie in the interval $[c, d]$.

Let ε_y be the error in the Kalman filter estimate of a specified state y and let ℓ_y be the maximum tolerable absolute error for ε_y . Determine an upper bound on the *integrity risk*, $P(|\varepsilon_y| > \ell_y)$ for all $a \in [c, d]$.

COVARIANCE PROPAGATION WITH UNCERTAIN PARAMETERS

The Kalman filter uses state augmentation to account for correlated noise. The augmented measurement and state dynamic models are

$$\begin{aligned}\begin{bmatrix} \mathbf{x}_{k+1} \\ m_{k+1} \end{bmatrix} &= \begin{bmatrix} \mathbf{A}_k & \mathbf{0} \\ \mathbf{0} & \bar{a} \end{bmatrix} \begin{bmatrix} \mathbf{x}_k \\ m_k \end{bmatrix} + \begin{bmatrix} \mathbf{0} \\ \sigma_m(1 - \bar{a}^2)^{1/2} \end{bmatrix} w_k \\ z_k &= [\mathbf{C}_k \quad 1] \begin{bmatrix} \mathbf{x}_k \\ m_k \end{bmatrix} + r_k\end{aligned}\Rightarrow \begin{aligned}\begin{bmatrix} \mathbf{x}_{k+1} \\ m_{k+1} \end{bmatrix} &= \mathbf{F}_k \begin{bmatrix} \mathbf{x}_k \\ m_k \end{bmatrix} + \mathbf{G}w_k \\ z_k &= \mathbf{H}_k \begin{bmatrix} \mathbf{x}_k \\ m_k \end{bmatrix} + r_k\end{aligned}\tag{3}$$

such that \bar{a} is any value in $[c, d]$ chosen by the filter designer. The Kalman filter covariance matrix accurately describes the estimate error statistics when $a = \bar{a}$. However, it is more common that $a \neq \bar{a}$. In this case, new estimate error equations must be derived to properly determine the estimate error covariance matrix. For the linear system in Eq. (1), Appendix A shows that

$$\begin{aligned}\mathbf{e}_{k+1}^- &= \mathbf{F}_k \mathbf{e}_k^+ \\ \mathbf{e}_k^+ &= (\mathbf{I} - \mathbf{K}_k \mathbf{H}_k) \mathbf{e}_k^- + \mathbf{K}_k v_k\end{aligned}\tag{4}$$

with $\mathbf{e}_k^T = [\boldsymbol{\varepsilon}_{x,k}^T \quad \hat{m}_k]$ and \mathbf{K}_k being the Kalman gain matrix. Notice that \mathbf{e}_k is driven by the correlated noise sequence v_k . Therefore, $E[\mathbf{e}_k^+ v_k] \neq \mathbf{0}$ and the covariance of \mathbf{e}_k cannot be updated recursively. To address this difficulty, substitute $v_k = m_k + r_k$ into Eq. (4) and incorporate the dynamic model from Eq. (2), resulting in the augmented system

$$\begin{aligned}
\begin{bmatrix} \mathbf{e}_{k+1}^- \\ m_{k+1} \end{bmatrix} &= \begin{bmatrix} \mathbf{F}_k & \mathbf{0} \\ \mathbf{0} & a \end{bmatrix} \begin{bmatrix} \mathbf{e}_k^+ \\ m_k \end{bmatrix} + \begin{bmatrix} \mathbf{0} \\ \sigma_m(1-a^2)^{1/2} \end{bmatrix} w_k &\Rightarrow \begin{aligned} \xi_{k+1}^- &= \mathbf{\Phi}_k \xi_k^+ + \mathbf{\Gamma} w_k \\ \xi_k^+ &= \mathbf{\Lambda}_k \xi_k^- + \mathbf{\Psi}_k r_k \end{aligned} \\
\begin{bmatrix} \mathbf{e}_k^+ \\ m_k \end{bmatrix} &= \begin{bmatrix} \mathbf{I} - \mathbf{K}_k \mathbf{H}_k & \mathbf{K}_k \\ \mathbf{0} & 1 \end{bmatrix} \begin{bmatrix} \mathbf{e}_k^- \\ m_k \end{bmatrix} + \begin{bmatrix} \mathbf{K}_k \\ 0 \end{bmatrix} r_k
\end{aligned} \tag{5}$$

where $\xi_k^T = [\mathbf{\varepsilon}_{x,k}^T \quad \hat{m}_k \quad m_k]$. This process is similar to the approach outlined in Section 7.2 of [6]. The covariance matrix of ξ_k propagates as

$$\begin{aligned}
\Sigma_{k+1}^- &= \mathbf{\Phi}_k \Sigma_k^+ \mathbf{\Phi}_k^T + \mathbf{\Gamma} \mathbf{\Gamma}^T \\
\Sigma_k^+ &= \mathbf{\Lambda}_k \Sigma_k^- \mathbf{\Lambda}_k^T + \mathbf{\Psi}_k \mathbf{\Psi}_k^T \sigma_r^2
\end{aligned} \tag{6}$$

Initialization

The initial covariance matrix is formally defined as

$$\Sigma_0^+ = E \left\{ \begin{bmatrix} \mathbf{\varepsilon}_{x,0}^+ \\ \hat{m}_0^+ \\ m_0 \end{bmatrix} [(\mathbf{\varepsilon}_{x,0}^+)^T \quad \hat{m}_0^+ \quad m_0] \right\} \tag{7}$$

It is customary to set $\hat{m}_0^+ = E[m_0]$. For the first order Gauss-Markov process, $E[m_k] = 0$ for all k . Thus, $\hat{m}_0^+ = 0$ and any expected values involving \hat{m}_0^+ are equal to 0. Expanding the right-hand side of Eq. (7) results in

$$\Sigma_0^+ = \begin{bmatrix} E[\mathbf{\varepsilon}_{x,0}^+(\mathbf{\varepsilon}_{x,0}^+)^T] & \mathbf{0} & E[\mathbf{\varepsilon}_{x,0}^+ m_0] \\ \mathbf{0} & 0 & 0 \\ E[m_0(\mathbf{\varepsilon}_{x,0}^+)^T] & 0 & E[m_0^2] \end{bmatrix} = \begin{bmatrix} \mathbf{P}_{x,0}^+ & \mathbf{0} & E[\mathbf{\varepsilon}_{x,0}^+ m_0] \\ \mathbf{0} & 0 & 0 \\ E[m_0(\mathbf{\varepsilon}_{x,0}^+)^T] & 0 & \sigma_m^2 \end{bmatrix} \tag{8}$$

During initialization, it's possible that $\mathbf{\varepsilon}_{x,0}^+$ and $\varepsilon_{m,0}^+$ are correlated. This happens for example when position states in a navigation Kalman filter are initialized using a least squares GPS solution. In this case, the initial estimate error $\mathbf{\varepsilon}_{x,0}^+$ is correlated with the GPS measurement errors. Notice that $E[\mathbf{\varepsilon}_{x,0}^+ \varepsilon_{m,0}^+] = E[\mathbf{\varepsilon}_{x,0}^+ (m_0 - \hat{m}_0^+)] = E[\mathbf{\varepsilon}_{x,0}^+ m_0]$. Defining $\mathbf{P}_{xm,0}^+ = E[\mathbf{\varepsilon}_{x,0}^+ \varepsilon_{m,0}^+]$, the initial covariance matrix is

$$\Sigma_0^+ = \begin{bmatrix} \mathbf{P}_{x,0}^+ & \mathbf{0} & \mathbf{P}_{xm,0}^+ \\ \mathbf{0} & 0 & 0 \\ (\mathbf{P}_{xm,0}^+)^T & 0 & \sigma_m^2 \end{bmatrix} \tag{9}$$

$\mathbf{P}_{x,0}^+$ and $\mathbf{P}_{xm,0}^+$ are application dependent and their determination will not be considered in this paper.

For Gaussian $\varepsilon_{y,k}$ (which is the case here given that v_k is Gaussian and the Kalman filter is a linear estimator), an upper bound on the integrity risk for y is equivalent to an upper bound on $\sigma_{y,k}^2$. Matrices $\mathbf{\Phi}_k$ and $\mathbf{\Gamma}$ are functions of a . One approach for maximizing $\sigma_{y,k}^2$ is to run multiple instantiations of Eq. (6) using different values of a . Gelb uses this philosophy in [6] to perform sensitivity analysis for the Kalman filter. In addition to running Eq. (6) multiple times, the authors in [7] also execute a bank of Kalman filters using different values of \bar{a} . Their goal was to determine the minimum upper bound on $\sigma_{y,k}^2$. These methods are useful for performing off-line analysis. As a method for real-time bounding of $\sigma_{y,k}^2$, they are only suitable for problems where the unknown parameters take on discrete values in the uncertainty interval. For continuously varying parameters, the brute force approach only makes sense if the number of parameters is low and the width of the uncertainty intervals is very small. There are few if any navigation applications satisfying these criteria. Multiple satellites and sensors are commonly used for state estimation, each having at least one uncertain error model parameter. In addition, measurement errors usually have a continuous distribution and do not cluster into distinct groups. Thus, parameter uncertainty is almost always continuous. The remainder of the paper focuses on addressing these practical difficulties and developing a new method to efficiently upper bound $\sigma_{y,k}^2$ that's applicable to multi-sensor navigation problems with continuously varying parameters.

EXACT SOLUTION FOR VARIANCE MAXIMIZATION

The estimate error covariance matrix is a polynomial function of a , which is most easily seen by propagating Eq. (4). Let $\mathbf{S}_k = \mathbf{I} - \mathbf{K}_k \mathbf{H}_k$. Through successive substitution, \mathbf{e}_k progresses as

$$\begin{aligned}
 \mathbf{e}_1^- &= \mathbf{F}_0 \mathbf{e}_0^+ \\
 \mathbf{e}_1^+ &= \mathbf{S}_1 \mathbf{F}_0 \mathbf{e}_0^+ + \mathbf{K}_1 \mathbf{v}_1 \\
 \mathbf{e}_2^- &= \mathbf{F}_1 (\mathbf{S}_1 \mathbf{F}_0 \mathbf{e}_0^+ + \mathbf{K}_1 \mathbf{v}_1) \\
 \mathbf{e}_2^+ &= \mathbf{S}_2 (\mathbf{F}_1 \mathbf{S}_1 \mathbf{F}_0 \mathbf{e}_0^+ + \mathbf{F}_1 \mathbf{K}_1 \mathbf{v}_1) + \mathbf{K}_2 \mathbf{v}_2 \\
 &\vdots
 \end{aligned} \tag{10}$$

Focusing on \mathbf{e}_k^+ , the general expression is

$$\begin{aligned}
 \mathbf{e}_k^+ &= \mathbf{B}_0 \mathbf{e}_0^- + \mathbf{b}_1 \mathbf{v}_1 + \mathbf{b}_2 \mathbf{v}_2 + \cdots + \mathbf{b}_k \mathbf{v}_k \\
 &= \mathbf{B}_0 \mathbf{e}_0^- + \mathbf{B}_{1:k} \mathbf{v}_{1:k}
 \end{aligned} \tag{11}$$

For $k = 2$, Eq. (10) shows that $\mathbf{B}_0 = \mathbf{S}_2 \mathbf{F}_1 \mathbf{S}_1 \mathbf{F}_0$, $\mathbf{B}_{1:2} = [\mathbf{S}_2 \mathbf{F}_1 \mathbf{K}_1 \quad \mathbf{K}_2]$ and $\mathbf{v}_{1:2}^T = [\mathbf{v}_1 \quad \mathbf{v}_2]$. Figure 1 summarizes how \mathbf{B}_0 and $\mathbf{B}_{1:k}$ are created in parallel with the Kalman filter covariance propagation.

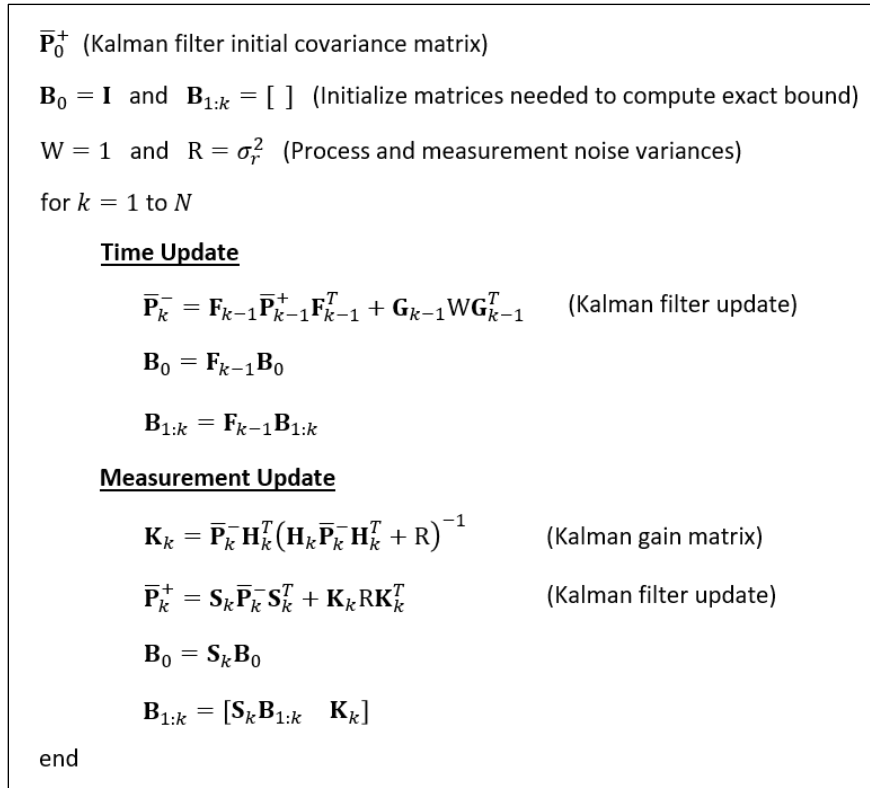


Figure 1. Pseudocode to generate matrices that define the exact polynomial coefficients.

The variance of $y_k = \alpha^T \mathbf{e}_k$ is given by

$$\sigma_{y,k}^2 = \alpha^T \mathbf{B}_0 \mathbf{P}_0^+ \mathbf{B}_0^T \alpha + \alpha^T \mathbf{B}_{1:k} E[\mathbf{v}_{1:k} \mathbf{v}_{1:k}^T] \mathbf{B}_{1:k}^T \alpha \tag{12}$$

Using the same approach to defining Σ_0^+ , the initial covariance matrix $\mathbf{P}_0^+ = E[\mathbf{e}_0^+(\mathbf{e}_0^+)^T] = \begin{bmatrix} \mathbf{P}_{x,0}^+ & \mathbf{0} \\ \mathbf{0} & 0 \end{bmatrix}$. Recalling that $v_k = m_k + r_k$ and using the fact that $E[m_i m_j] = \sigma_m^2 a^{|i-j|}$ and $E[r_i r_j] = \sigma_r^2 \delta(i-j)$,

$$E[\mathbf{v}_{1:k} \mathbf{v}_{1:k}^T] = (\sigma_r^2 + \sigma_m^2) \mathbf{I} + \sigma_m^2 \begin{bmatrix} 0 & a & a^2 & \dots & a^{k-1} \\ a & 0 & a & \ddots & \vdots \\ a^2 & a & 0 & \ddots & a^2 \\ \vdots & \ddots & \ddots & \ddots & a \\ a^{k-1} & \dots & a^2 & a & 0 \end{bmatrix} \quad (13)$$

Substituting Eq. (13) into Eq. (12) and reordering results in the polynomial

$$\sigma_{y,k}^2 = \boldsymbol{\alpha}^T [\mathbf{B}_0 \mathbf{P}_0^+ \mathbf{B}_0^T + (\sigma_r^2 + \sigma_m^2) \mathbf{B}_{1:k} \mathbf{B}_{1:k}^T] \boldsymbol{\alpha} + 2\sigma_m^2 \sum_{i=1}^{k-1} \text{sum}[\text{diag}(\mathbf{B}_{1:k}^T \boldsymbol{\alpha} \boldsymbol{\alpha}^T \mathbf{B}_{1:k}, i)] a^i \quad (14)$$

where the notation $\text{sum}[\text{diag}(\mathbf{A}, i)]$ denotes the sum of elements along the i^{th} super-diagonal of \mathbf{A} . The maximum value of $\sigma_{y,k}^2$ occurs at an endpoint of the feasible interval or at a critical point where $d\sigma_{y,k}^2/da = 0$.

This process provides an exact solution to the integrity risk bounding problem, but has two deficiencies: it requires storage of the matrix $\mathbf{M} = \mathbf{B}_{1:k}^T \boldsymbol{\alpha} \boldsymbol{\alpha}^T \mathbf{B}_{1:k}$ that grows with each new measurement, and it requires finding all the roots of a polynomial whose order increases without bound. As a specific example, consider the scenario of running a Kalman filter with a 100 Hz sensor. After 5 minutes of filtering, $\mathbf{B}_{1:k}$ will have 30,000 columns and \mathbf{M} will have 9×10^8 elements. Assuming double precision (8 bytes per matrix element), \mathbf{M} would occupy 7.2 gigabytes of memory. Determining the maximum value of $\sigma_{y,k}^2$ requires finding all roots of a 29,999-order polynomial. This example illustrates that the exact solution only makes sense for short duration applications with a maximum time dependent on sensor sampling rates.

APPROXIMATE VARIANCE BOUND USING TAYLOR SERIES

This section derives an approximate integrity risk bound by expanding $\sigma_{y,k}^2$ in a Taylor series. While it's almost trivial to form the series once the polynomial coefficients have been determined, we seek a better approach that does not require storing \mathbf{M} .

To begin, notice from Eq. (5) that Φ_k is linear in a and $\Gamma \Gamma^T$ is quadratic in a . Successive derivatives of Φ_k and $\Gamma \Gamma^T$ are

$$\frac{d^i \Phi_k}{da^i} = \begin{cases} \begin{bmatrix} \mathbf{0} & \mathbf{0} \\ \mathbf{0} & \mathbf{1} \end{bmatrix} & \text{if } i = 1 \\ \begin{bmatrix} \mathbf{0} & \mathbf{0} \\ \mathbf{0} & \mathbf{0} \end{bmatrix} & \text{if } i \geq 1 \end{cases} \quad (15)$$

and

$$\frac{d^i (\Gamma \Gamma^T)}{da^i} = \begin{cases} \begin{bmatrix} \mathbf{0} & \mathbf{0} \\ \mathbf{0} & -2\sigma_m^2 a \end{bmatrix} & \text{if } i = 1 \\ \begin{bmatrix} \mathbf{0} & \mathbf{0} \\ \mathbf{0} & -2\sigma_m^2 \end{bmatrix} & \text{if } i = 2 \\ \begin{bmatrix} \mathbf{0} & \mathbf{0} \\ \mathbf{0} & \mathbf{0} \end{bmatrix} & \text{if } i \geq 2 \end{cases} \quad (16)$$

The covariance matrix after a time update was shown in Eq. (6) to be $\Sigma_{k+1}^- = \Phi_k \Sigma_k^+ \Phi_k^T + \Gamma \Gamma^T$. Let $\mathbf{x}^{(i)}$ be the i^{th} derivative of \mathbf{x} with respect to a . Then for $i = 1$

$$(\Sigma_{k+1}^-)^{(1)} = (\Phi_k \Sigma_k^+)^{(1)} + [\Phi_k (\Sigma_k^+)^{(1)} + (\Phi_k)^{(1)} \Sigma_k^+] \Phi_k^T + (\Gamma \Gamma^T)^{(1)} \quad (17)$$

With $i = 2$

$$\begin{aligned} (\Sigma_{k+1}^-)^{(2)} &= 2[\Phi_k(\Sigma_k^+)^{(1)} + (\Phi_k)^{(1)}\Sigma_k^+](\Phi_k^T)^{(1)} \\ &\quad + [\Phi_k(\Sigma_k^+)^{(2)} + 2(\Phi_k)^{(1)}(\Sigma_k^+)^{(1)}]\Phi_k^T + (\Gamma\Gamma^T)^{(2)} \end{aligned} \quad (18)$$

Continuing with $i = 3$

$$\begin{aligned} (\Sigma_{k+1}^-)^{(3)} &= 3[\Phi_k(\Sigma_k^+)^{(2)} + 2(\Phi_k)^{(1)}(\Sigma_k^+)^{(1)}](\Phi_k^T)^{(1)} \\ &\quad + [\Phi_k(\Sigma_k^+)^{(3)} + 3(\Phi_k)^{(1)}(\Sigma_k^+)^{(2)}]\Phi_k^T \end{aligned} \quad (19)$$

In general, the i^{th} derivative is

$$\begin{aligned} (\Sigma_{k+1}^-)^{(i)} &= i[\Phi_k(\Sigma_k^+)^{(i-1)} + (i-1)(\Phi_k)^{(1)}(\Sigma_k^+)^{(i-2)}](\Phi_k^T)^{(1)} \\ &\quad + [\Phi_k(\Sigma_k^+)^{(i)} + n(\Phi_k)^{(1)}(\Sigma_k^+)^{(i-1)}]\Phi_k^T \\ &\quad + (\Gamma\Gamma^T)^{(1)}\delta(i-1) + (\Gamma\Gamma^T)^{(2)}\delta(i-2) \end{aligned} \quad (20)$$

where $\delta(x)$ is the Kronecker delta. The covariance matrix after a measurement update is $\Sigma_k^+ = \Lambda_k \Sigma_k^- \Lambda_k^T + \Psi_k \Psi_k^T \sigma_r^2$. Given that Λ_k and Ψ_k are not functions of a , the i^{th} derivative of Σ_k^+ is

$$(\Sigma_k^+)^{(i)} = \Lambda_k (\Sigma_k^-)^{(i)} \Lambda_k^T \quad (21)$$

The i^{th} derivative term in the Taylor series is divided by $i!$. The factorial can be absorbed in the series coefficients by making the definition $\mathbf{D}_{i,k} = (1/i!)(\Sigma_k)^{(i)}$. Multiplying both sides of Eqs. (20) and (21) by $1/i!$ and simplifying yields

$$\begin{aligned} \mathbf{D}_{i,k+1}^- &= [\Phi_k \mathbf{D}_{i-1,k}^+ + (\Phi_k)^{(1)} \mathbf{D}_{i-2,k}^+](\Phi_k^T)^{(1)} + [\Phi_k \mathbf{D}_{i,k}^+ + (\Phi_k)^{(1)} \mathbf{D}_{i-1,k}^+]\Phi_k^T \\ &\quad + \frac{1}{i!} [(\Gamma\Gamma^T)^{(1)}\delta(i-1) + (\Gamma\Gamma^T)^{(2)}\delta(i-2)] \\ \mathbf{D}_{i,k}^+ &= \Lambda_k \mathbf{D}_{i,k}^- \Lambda_k^T \end{aligned} \quad (22)$$

Given an expansion point a^* , the N^{th} order Taylor series approximation of Σ_k is

$$\Sigma_k \approx \Sigma_k^* + \sum_{i=1}^N \mathbf{D}_{i,k}^* (a - a^*)^i \quad (23)$$

If $a^* = \bar{a}$, then Σ_k^* is equivalent to the Kalman filter covariance matrix. Figure 2 summarizes the algorithm for Taylor series propagation.

For the specified state $y_k = \beta^T \xi_k$, the Taylor polynomial for $\sigma_{y,k}^2$ is

$$s_{y,k}^2 \approx \beta^T \Sigma_k^* \beta + \sum_{n=1}^N \beta^T \mathbf{D}_{n,k}^* \beta (a - a^*)^n \quad (24)$$

Equation (24) is a polynomial in the unknown variable $\delta a = a - a^*$. With $a \in [c, d]$, the feasible region of δa is $[c - a^*, d - a^*]$. The maximum value of $s_{y,k}^2$ occurs at an endpoint of the feasible region or at a critical point where $ds_{y,k}^2/d(\delta a) = 0$.

```

 $\bar{\mathbf{P}}_0^+$  (Kalman filter initial covariance matrix)
 $\mathbf{\Sigma}_0^+$  (Initial covariance matrix of  $\xi_0^+$ )
 $W = 1$  and  $R = \sigma_r^2$  (Process and measurement noise variances)
for  $k = 1$  to  $K$ 
  Time Update
     $\bar{\mathbf{P}}_k^- = \mathbf{F}_{k-1} \bar{\mathbf{P}}_{k-1}^+ \mathbf{F}_{k-1}^T + \mathbf{G}_{k-1} \mathbf{W} \mathbf{G}_{k-1}^T$ 
     $\mathbf{\Sigma}_k^- = \mathbf{\Phi}_{k-1} \mathbf{\Sigma}_{k-1}^+ \mathbf{\Phi}_{k-1}^T + \mathbf{\Gamma} \mathbf{W} \mathbf{\Gamma}^T$ 
     $\mathbf{D}_{-1,k-1}^+ = [ ]$  and  $\mathbf{D}_{0,k-1}^+ = \mathbf{\Sigma}_{k-1}^+$ 
    for  $i = 1$  to  $N$ 
       $\mathbf{D}_{i,k}^- = \left( \mathbf{\Phi}_{k-1} \mathbf{D}_{i-1,k-1}^+ + \mathbf{\Phi}_{k-1}^{(1)} \mathbf{D}_{i-2,k-1}^+ \right) \left( \mathbf{\Phi}_{k-1}^T \right)^{(1)} + \left( \mathbf{\Phi}_{k-1} \mathbf{D}_{i,k-1}^+ + \mathbf{\Phi}_{k-1}^{(1)} \mathbf{D}_{i-1,k-1}^+ \right) \mathbf{\Phi}_{k-1}^T$ 
       $+ \frac{1}{i!} \left[ (\mathbf{\Gamma} \mathbf{\Gamma}^T)^{(1)} \delta(i-1) + (\mathbf{\Gamma} \mathbf{\Gamma}^T)^{(2)} \delta(i-2) \right]$ 
    end
  Measurement Update
     $\mathbf{K}_k = \bar{\mathbf{P}}_k^- \mathbf{H}_k^T \left( \mathbf{H}_k \bar{\mathbf{P}}_k^- \mathbf{H}_k^T + R \right)^{-1}$ 
     $\bar{\mathbf{P}}_k^+ = \mathbf{S}_k \bar{\mathbf{P}}_k^- \mathbf{S}_k^T + \mathbf{K}_k \mathbf{R} \mathbf{K}_k^T$ 
     $\mathbf{\Sigma}_k^+ = \mathbf{\Lambda}_k \mathbf{\Sigma}_k^- \mathbf{\Lambda}_k^T + \mathbf{K}_k \mathbf{R} \mathbf{K}_k^T$ 
    for  $i = 1$  to  $N$ 
       $\mathbf{D}_{i,k}^+ = \mathbf{\Lambda}_k \mathbf{D}_{i,k}^- \mathbf{\Lambda}_k^T$ 
    end
end
end

```

Figure 2. Pseudocode to generate matrices that define the Taylor polynomial coefficients.

Comparing Eq. (24) to the expression for $\sigma_{y,k}^2$ (reproduced below) highlights the contribution in this paper.

$$\sigma_{y,k}^2 = \boldsymbol{\alpha}^T [\mathbf{B}_0 \mathbf{P}_0^+ \mathbf{B}_0^T + (\sigma_r^2 + \sigma_m^2) \mathbf{B}_{1:k} \mathbf{B}_{1:k}^T] \boldsymbol{\alpha} + 2\sigma_m^2 \sum_{i=1}^{k-1} \text{sum}[\text{diag}(\mathbf{B}_{1:k}^T \boldsymbol{\alpha} \boldsymbol{\alpha}^T \mathbf{B}_{1:k}, i)] a^i$$

The most notable difference between the two expressions is how polynomial coefficients are computed. For the exact expression, there is no way to take advantage of previous calculations. Thus, the coefficients must be recomputed from scratch at every time index k . The matrix $\mathbf{B}_{1:k}$ (which acquires a new column as k increases) keeps track of the entire measurement sequence's effect on the estimate error covariance matrix. Using a Taylor series approximation allows the polynomial coefficients to be updated recursively and involves fixed size matrices. Loosely speaking, $\mathbf{B}_{1:k}$ is replaced by $\mathbf{D}_{n,k}^*$. The other distinct difference between the two representations is the order of the polynomial, which dictates how quickly variance maximization can take place. The critical points are determined by finding all roots of the variance polynomial. Because the order of the exact polynomial grows linearly without bound, it takes progressively longer to determine critical points. The Taylor polynomial has a fixed order that is likely much lower than the order of the exact expression, enabling critical points to be computed quickly regardless of how long the Kalman filter has been running. The algorithms developed in this paper make it possible to compute a real-time upper bound on integrity risk for a wide range of navigation applications, something that has remained elusive until now.

TAYLOR REMAINDER THEOREM

An open question is how to determine the order of the Taylor series, n . The Taylor remainder theorem is often used to set n . For an arbitrary function $f(a)$, the integral form of the remainder theorem states that [8]

$$R_{n,a^*}(a) = f(a) - T_n(a) = \int_{a^*}^a \frac{f^{(n+1)}(u)}{n!} (a-u)^n du \quad (25)$$

where a^* is the expansion point and $T_n(a)$ is the n^{th} order Taylor polynomial for $f(a)$.

In this paper, $f(a)$ is the estimate error variance polynomial. The last section showed that it was not practical to keep track of $f(a)$, and instead $f(a)$ is known only by its Taylor series approximation. This presents a unique problem, because clearly the Taylor series cannot be used to quantify the error in the Taylor series (this would result in $R_{n,a^*}(a) = 0$, which is obviously not correct). One solution is to use an N^{th} order Taylor series to quantify the error in the n^{th} order expansion, where $n < N$. For this approach to make sense, there must be good separation between n and N to ensure that $f^{(n+1)}(u)$ is adequately described.

Additional margin is built in if the remainder is computed for an m^{th} order Taylor series such that $m < n$. As a specific example, suppose that a 15th order Taylor series is formed and the 10th order polynomial is used to maximize the variance (i.e., $N = 15$ and $n = 10$). The 11th order derivative is needed to quantify the error in the Taylor approximation. A 4th order polynomial may not be sufficient to describe the 11th derivative of $f(a)$. Instead, we can assume that $m = 5$, resulting in a 9th order approximation for the 6th derivative. A higher order expansion is preferable, and any residual error in approximating the derivative is likely going to be absorbed in the margin introduced from computing $R_{5,a^*}(a)$ instead of $R_{10,a^*}(a)$. See Appendix B for a closed form expression for $R_{n,a^*}(a)$.

The remainder theorem is used in this paper to introduce conservatism and provide justification that the approximate variance bound is larger than the exact bound. Using \tilde{a} to denote the parameter value producing the maximum variance, the approximate bound is modified according to

$$\bar{s}_{y,k}^2 = s_{y,k}^2(\tilde{a}) + |R_{m,a^*}(\tilde{a})| \quad (26)$$

Rather than defining N to achieve a specified accuracy, N is chosen to ensure that the remainder term is sufficiently resolved and that m is large enough to reduce conservatism in $\bar{s}_{y,k}^2$. The steps involved in forming $\bar{s}_{y,k}^2$ are summarized in Figure 3.

- (1) Use the algorithm in Figure 2 to form the Taylor polynomial, $s_{y,k}^2(a)$.
- (2) Determine \tilde{a} , the parameter value that maximizes $s_{y,k}^2(a)$.
- (3) Evaluate the remainder, $R_{m,a^*}(\tilde{a})$ using the result in Appendix B.
- (4) Compute variance bound, $\bar{s}_{y,k}^2 = s_{y,k}^2(\tilde{a}) + |R_{m,a^*}(\tilde{a})|$.

Figure 3. Algorithm outline for computing conservative upper bound on estimate error variance.

The remainder in Eq. (26) assumes that \tilde{a} is the true location of the maximum variance. In general, this is not the case because maximization is done based on a Taylor approximation. Figure 4 shows that if margin is not included when computing the remainder, it is possible that $\bar{s}_{y,k}^2$ will be smaller than the true maximum variance.

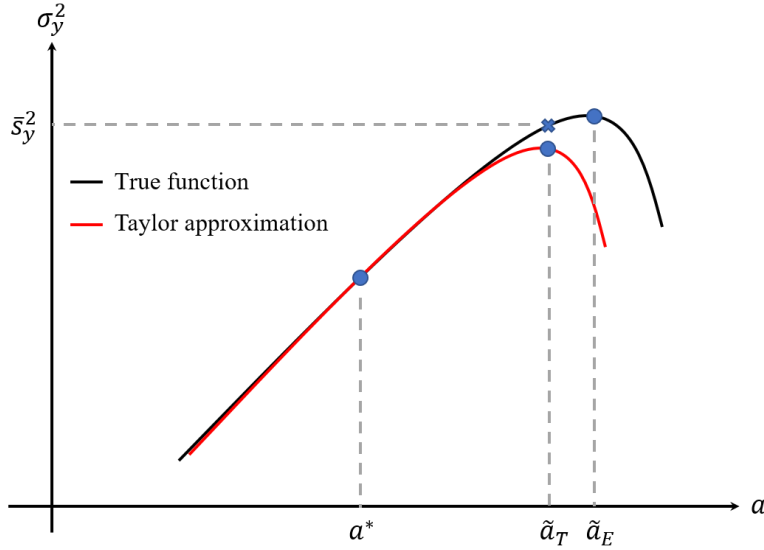


Figure 4. Maximizing the variance using the true vs. approximate function.

Figure 4 is a conceptual illustration, and it is expected that the real curves will be nearly coincident. While it seems reasonable that the conservatism introduced from computing the remainder for a lower order approximation will account for the situation in Figure 4, there is no guarantee. Ideally, the maximum remainder should be used in Eq. (27), which would ensure that $\bar{\sigma}_{y,k}^2$ is a true upper bound. This is a topic for future work.

ILLUSTRATIVE EXAMPLE

The methods developed earlier are applied to the one-dimensional navigation problem in Figure 5.

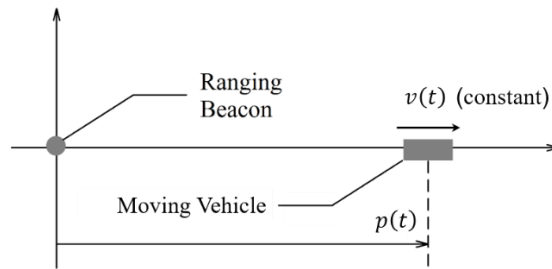


Figure 5. One-dimensional navigation problem.

A Kalman filter is used to estimate a vehicle's position p and speed v along the x -axis using measurements of position from a ranging beacon at the origin. The beacon measurement interval is $\Delta t = 1$ sec and the vehicle is known to be traveling at constant speed.

With $\mathbf{x}_k^T = [p_k \quad v_k]$, the measurement and state dynamic models are

$$\begin{aligned} \mathbf{x}_{k+1} &= \begin{bmatrix} 1 & \Delta t \\ 0 & 1 \end{bmatrix} \mathbf{x}_k & \Rightarrow & \mathbf{x}_{k+1} = \mathbf{A} \mathbf{x}_k \\ z_k &= [1 \quad 0] \mathbf{x}_k + m_k + r_k & & z_k = \mathbf{C} \mathbf{x}_k + m_k + r_k \end{aligned} \quad (27)$$

such that m_k is a first order Gauss-Markov process with variance σ_m^2 and r_k is zero-mean white Gaussian noise with variance σ_r^2 .

Throughout the paper, the dynamic model for m_k was written as $m_{k+1} = am_k + \sigma_m(1 - a^2)^{1/2} w_k$. For the first order Gauss-Markov process, it is well known that $a = \exp(-\Delta t/\tau)$, where τ is the time constant of the process [6]. This substitution will be made because it's easier to visualize results using τ and because it's more common to specify uncertainty on τ rather than a . Table 1 summarizes the error model parameters.

Table 1. Ranging beacon error model parameters.

White noise standard deviation (σ_r)	0.5 meters
Gauss-Markov standard deviation (σ_m)	1 meter
Gauss-Markov time constant (τ)	Between 50 and 300 seconds

The Kalman filter is a 3-state filter that uses state augmentation to estimate m_k in addition to p_k and v_k . The state-augmented models are

$$\begin{aligned} \begin{bmatrix} \mathbf{x}_{k+1} \\ m_{k+1} \end{bmatrix} &= \begin{bmatrix} \mathbf{A} & \mathbf{0} \\ \mathbf{0} & e^{-\Delta t/\bar{\tau}} \end{bmatrix} \begin{bmatrix} \mathbf{x}_k \\ m_k \end{bmatrix} + \begin{bmatrix} 0 \\ \sigma_m(1 - e^{-2\Delta t/\bar{\tau}})^{1/2} \end{bmatrix} w_k \\ z_k &= [\mathbf{C} \quad 1] \begin{bmatrix} \mathbf{x}_k \\ m_k \end{bmatrix} + r_k \end{aligned} \tag{28}$$

and the initial covariance matrix is $\mathbf{P}_0^+ = \text{diag}[(10 \text{ m})^2, (1 \text{ m/s})^2, \sigma_m^2]$. Any value $\bar{\tau} \in [50, 300]$ can be used to define the filter. For this example, $\bar{\tau} = 300$ seconds is used in accordance with the notion that assuming maximum correlation should produce an upper bound on the estimate error variance. This hypothesis is tested by propagating Eq. (6) using multiple time constants over the admissible range. The results are shown in Figure 6 for the position state.

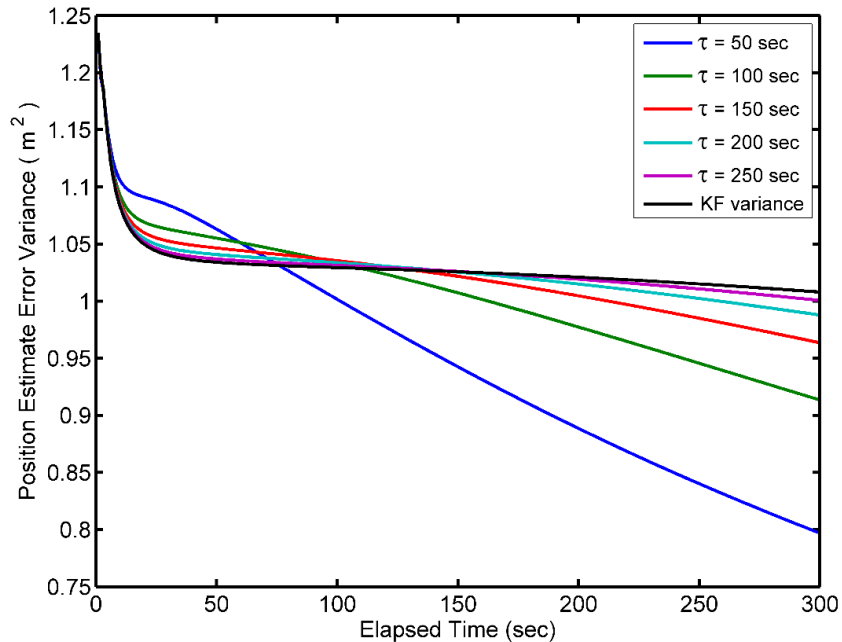


Figure 6. Position estimate error variance as a function of true time constant, τ .

The black line is the estimate error variance predicted by the Kalman filter. All other lines depict the true estimate error variance when the beacon measurement noise has a time constant τ , but the filter assumes the time constant is 300 seconds. The most striking result is that the KF variance does not always upper bound the true variance, even though it is based on an error model

assuming maximum correlation. Another interesting observation is that the worst-case behavior changes over time. At an elapsed time of 25 seconds, the position estimate error variance is largest when the beacon measurement noise has the least amount of time correlation ($\tau = 50$ seconds). The complete opposite is true after 250 seconds of filtering; the maximum variance occurs when measurement noise samples are highly correlated.

Figure 7 shows the results produced by the exact bounding algorithm. As expected, the variance bound is an upper envelope on the set of covariance propagations obtained using all time constants in the admissible interval. The time constant producing the variance bound transitions from the lower limit of 50 seconds to the upper limit of 300 seconds, which is consistent with the results in Figure 6. Notice the drop from 300 seconds to 50 seconds that occurs at the beginning of Figure 7b. This is due to a sharp change in the variance polynomial's behavior. Figure 8 provides a side-by-side comparison after the third and fourth measurements.

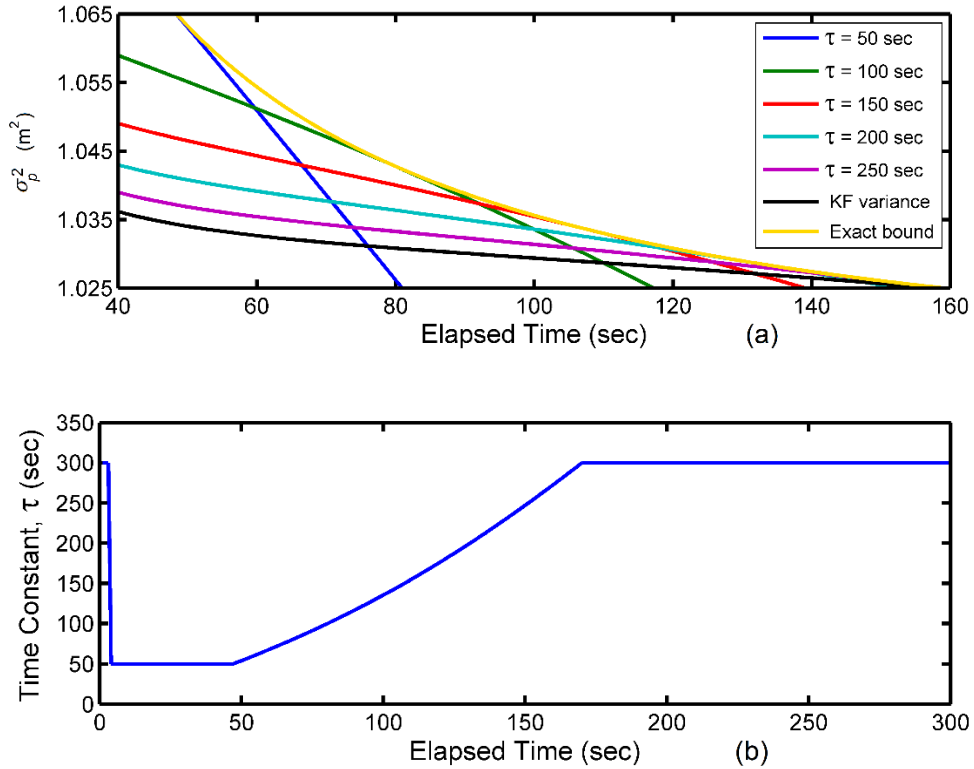
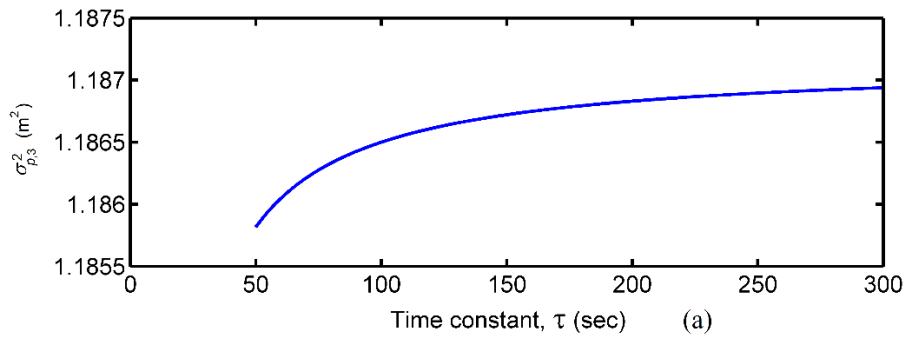


Figure 7. Output from exact bounding algorithm: (a) variance bound as the upper envelope of an ensemble of covariance propagations and (b) value of τ producing the maximum variance.



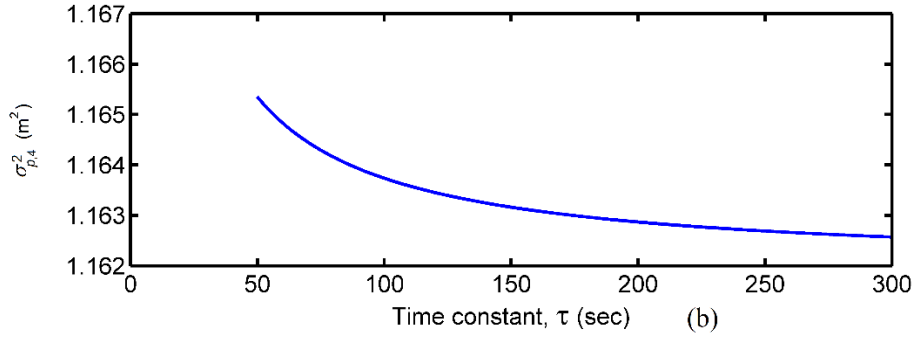


Figure 8. Variance polynomial as a function of τ after (a) three beacon measurements and (b) four beacon measurements.

There are many observations that beg for a physical explanation. Why does the variance polynomial suddenly change behavior after 3 measurements? What is significant about an elapsed time of 50 seconds, at which point the worst-case time constant in Figure 7b begins to rise? Is it related to the lower limit on τ ? What controls how quickly the time constant rises in Figure 7b? The stark reality is that there likely is no physical explanation for this behavior. We simply must accept that Kalman filters do not behave intuitively in the presence of measurement error model uncertainty. There are no simple rules to guide the design of a Kalman filter that guarantees an upper bound on integrity risk. The algorithms developed in this paper must therefore be used to ensure navigation system integrity. Thus, it is critical that they are efficient and able to operate in real-time.

The behavior of the approximate bounding method is observed under the conditions in Table 2.

Table 2. Error model parameters.

Taylor polynomial order (N)	15
Polynomial order for variance maximization (n)	5 through 8
Polynomial order for remainder calculation (m)	5
Expansion point (a^*)	$\frac{1}{2} \left(e^{-\frac{\Delta t}{50}} + e^{-\frac{\Delta t}{300}} \right)$

The expansion point is chosen to be the midpoint of the uncertainty interval for $a = \exp(-\Delta t/\tau)$. Figure 9 quantifies the approximate bound as a percent increase in the exact bound.

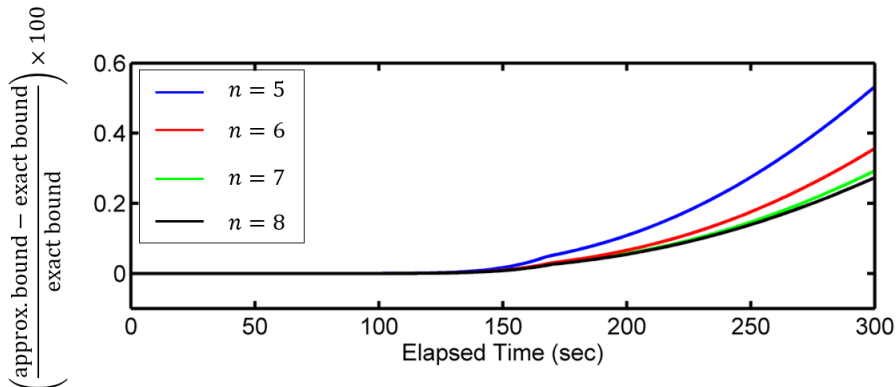


Figure 9. Approximate bound as a percent increase in the exact bound.

The percent increase is positive for all cases considered, indicating that the approximate bound is conservative. Figure 9 also shows that the bound is very tight and is at most 0.5% larger than the exact bound. The fact that these results have been obtained using low order polynomials for variance maximization is very encouraging. It strongly suggests that the algorithms developed in this paper can provide a real-time, tight upper bound on integrity risk for Kalman filters with uncertain measurement error models.

CONCLUSION

In this paper, a new approach was presented to upper bound integrity risk for the Kalman filter when the measurement noise autocorrelation function has parametric uncertainty. Drawing on existing literature, an augmented state model was first developed to express the true estimate error covariance matrix in terms of the uncertain parameter. It was shown that the error variance for a specified state is a polynomial function of the parameter whose order grows without bound. A recursive algorithm was derived to propagate the Taylor series coefficients of the variance polynomial. An upper bound on integrity risk was then defined in terms of the maximum value of the Taylor polynomial. Using the Taylor remainder theorem, a methodology was established to introduce conservatism in the approximate bound. For a one-dimensional estimation problem, it was shown that the algorithms derived in this paper provide a tight upper bound on integrity risk and require less than 10 terms in the Taylor series expansion. The approach described herein represents a significant improvement over existing methods and for the first time provides the ability to compute a tight upper bound on integrity risk for the Kalman filter in real-time. Future topics include applying this new approach to representative multi-sensor navigation applications. Additional work is also warranted in determining the maximum value of the Taylor remainder, which would further substantiate that the approximate bound is at least as large as the exact bound.

REFERENCES

- [1] B. DeCleene, "Defining Pseudorange Integrity-Overbounding," *Proceedings of the 13th International Technical Meeting of the Satellite Division of the Institute of Navigation*, pp. 1916-1924, Sept., 2000.
- [2] J. Rife, S. Pullen, B. Pervan, and P. Enge, "Paired Overbounding and Application to GPS Augmentation," *Proceedings of the IEEE Position, Location and Navigation Symposium*, pp. 439-446, April, 2004.
- [3] J. Rife and D. Gebre-Egziabher, "Symmetric Overbounding of Correlated Errors," *NAVIGATION*, vol. 54, no. 2, pp. 109-124, 2007.
- [4] G. W. Pulford, "A Proof of the Spherically Symmetric Overbounding Theorem for Linear Systems," *NAVIGATION* vol. 55, no. 4, pp. 283-292, 2008.
- [5] S. Langel, S. Khanafseh and B. Pervan, "Bounding Integrity Risk for Sequential State Estimators with Stochastic Modeling Uncertainty," *AIAA J. of Guidance, Control and Dynamics*, vol. 37, no. 1, pp. 36-46, 2014.
- [6] A. Gelb, Ed., "Suboptimal Filter Design and Sensitivity Analysis," in *Applied Optimal Estimation*, Cambridge, MA: The MIT Press, 1974, ch. 7, pp. 229-276.
- [7] S. Khanafseh, S. Langel and B. Pervan, "Overbounding Position Errors in the Presence of Carrier Phase Multipath Error Model Uncertainty," *Proceedings of the IEEE/ION Position, Location and Navigation Symposium*, pp. 575-584, May, 2010.
- [8] H. H. Sohrab, "The Riemann Integral," in *Basic Real Analysis*, 2nd ed., New York: Springer, 2014, ch. 7, pp. 329-330.
- [9] I. S. Gradshteyn and I. M. Ryzhik, *Table of Integrals, Series, and Products*, 7th ed., Boston: Elsevier, 2007.

APPENDIX A

For the state-augmented system in Eq. (3), the Kalman filter produces the following estimates of $\begin{bmatrix} \mathbf{x}_k \\ m_k \end{bmatrix}$

$$\begin{bmatrix} \hat{\mathbf{x}}_{k+1}^- \\ \hat{m}_{k+1}^- \end{bmatrix} = \begin{bmatrix} \mathbf{A}_k & \mathbf{0} \\ \mathbf{0} & \bar{a} \end{bmatrix} \begin{bmatrix} \hat{\mathbf{x}}_k^+ \\ \hat{m}_k^+ \end{bmatrix} \quad (\text{A1})$$

$$\begin{bmatrix} \hat{\mathbf{x}}_k^+ \\ \hat{m}_k^+ \end{bmatrix} = \begin{bmatrix} \hat{\mathbf{x}}_k^- \\ \hat{m}_k^- \end{bmatrix} + \mathbf{K}_k \left(z_k - [\mathbf{C}_k \quad 1] \begin{bmatrix} \hat{\mathbf{x}}_k^- \\ \hat{m}_k^- \end{bmatrix} \right) \quad (\text{A2})$$

The estimate error vector after a time update (Eq. (A1)) is usually derived by first subtracting $\begin{bmatrix} \mathbf{x}_{k+1} \\ \mathbf{m}_{k+1} \end{bmatrix}$ from both sides and incorporating the dynamic model on the right-hand side to align the time indices. That is

$$\begin{bmatrix} \widehat{\mathbf{x}}_{k+1}^- \\ \widehat{\mathbf{m}}_{k+1}^- \end{bmatrix} - \begin{bmatrix} \mathbf{x}_{k+1} \\ \mathbf{m}_{k+1} \end{bmatrix} = \begin{bmatrix} \mathbf{A}_k & \mathbf{0} \\ \mathbf{0} & \bar{a} \end{bmatrix} \begin{bmatrix} \widehat{\mathbf{x}}_k^+ \\ \widehat{\mathbf{m}}_k^+ \end{bmatrix} - \left\{ \begin{bmatrix} \mathbf{A}_k & \mathbf{0} \\ \mathbf{0} & a \end{bmatrix} \begin{bmatrix} \mathbf{x}_k \\ \mathbf{m}_k \end{bmatrix} + \begin{bmatrix} \mathbf{0} \\ \sigma_m(1-a^2)^{1/2} \end{bmatrix} \mathbf{w}_k \right\} \quad (\text{A3})$$

For the augmented state \mathbf{m}_k , Eq. (A3) indicates that

$$\varepsilon_{\mathbf{m},k+1}^- = \bar{a}\widehat{\mathbf{m}}_k^+ - a\mathbf{m}_k - \sigma_m(1-a^2)^{1/2}\mathbf{w}_k \quad (\text{A4})$$

Equation (A4) is a proper update equation only when $a = \bar{a}$. Because this paper is interested in $a \neq \bar{a}$, a different approach is adopted. Subtract $\begin{bmatrix} \mathbf{x}_{k+1} \\ \mathbf{0} \end{bmatrix}$ from both sides of the time update and incorporate the dynamic model for \mathbf{x}_k from Eq. (1) on the right-hand side

$$\begin{bmatrix} \widehat{\mathbf{x}}_{k+1}^- \\ \widehat{\mathbf{m}}_{k+1}^- \end{bmatrix} - \begin{bmatrix} \mathbf{x}_{k+1} \\ \mathbf{0} \end{bmatrix} = \begin{bmatrix} \mathbf{A}_k & \mathbf{0} \\ \mathbf{0} & \bar{a} \end{bmatrix} \begin{bmatrix} \widehat{\mathbf{x}}_k^+ \\ \widehat{\mathbf{m}}_k^+ \end{bmatrix} - \begin{bmatrix} \mathbf{A}_k & \mathbf{0} \\ \mathbf{0} & \mathbf{0} \end{bmatrix} \begin{bmatrix} \mathbf{x}_k \\ \mathbf{0} \end{bmatrix} \quad (\text{A5})$$

Defining $\mathbf{e}_k = \begin{bmatrix} \widehat{\mathbf{x}}_k - \mathbf{x}_k \\ \widehat{\mathbf{m}}_k \end{bmatrix} = \begin{bmatrix} \varepsilon_{\mathbf{x},k} \\ \widehat{\mathbf{m}}_k \end{bmatrix}$, Eq. (A5) takes the form

$$\mathbf{e}_{k+1}^- = \mathbf{F}_k \mathbf{e}_k^+ \quad (\text{A6})$$

Propagation of \mathbf{e}_k through the measurement update (Eq. (A2)) is obtained by substituting $z_k = \mathbf{C}_k \mathbf{x}_k + \mathbf{v}_k$ and subtracting $\begin{bmatrix} \mathbf{x}_k \\ \mathbf{0} \end{bmatrix}$ from both sides

$$\begin{bmatrix} \widehat{\mathbf{x}}_k^+ \\ \widehat{\mathbf{m}}_k^+ \end{bmatrix} - \begin{bmatrix} \mathbf{x}_k \\ \mathbf{0} \end{bmatrix} = \begin{bmatrix} \widehat{\mathbf{x}}_k^- \\ \widehat{\mathbf{m}}_k^- \end{bmatrix} - \begin{bmatrix} \mathbf{x}_k \\ \mathbf{0} \end{bmatrix} + \mathbf{K}_k \left(\begin{bmatrix} \mathbf{C}_k & \mathbf{1} \end{bmatrix} \begin{bmatrix} \mathbf{x}_k \\ \mathbf{0} \end{bmatrix} + \mathbf{v}_k - \begin{bmatrix} \mathbf{C}_k & \mathbf{1} \end{bmatrix} \begin{bmatrix} \widehat{\mathbf{x}}_k^- \\ \widehat{\mathbf{m}}_k^- \end{bmatrix} \right) \quad (\text{A7})$$

Recognizing that $\begin{bmatrix} \mathbf{C}_k & \mathbf{1} \end{bmatrix} = \mathbf{H}_k$, Eq. (A7) simplifies to

$$\mathbf{e}_k^+ = (\mathbf{I} - \mathbf{K}_k \mathbf{H}_k) \mathbf{e}_k^- + \mathbf{K}_k \mathbf{v}_k \quad (\text{A8})$$

Considering Eqs. (A6) and (A8) together, \mathbf{e}_k propagates through the Kalman filter according to

$$\begin{aligned} \mathbf{e}_{k+1}^- &= \mathbf{F}_k \mathbf{e}_k^+ \\ \mathbf{e}_k^+ &= (\mathbf{I} - \mathbf{K}_k \mathbf{H}_k) \mathbf{e}_k^- + \mathbf{K}_k \mathbf{v}_k \end{aligned} \quad (\text{A9})$$

APPENDIX B

This appendix provides a closed form expression for the Taylor remainder of an m^{th} expansion of the variance polynomial. The variance polynomial is approximated by its N^{th} order ($N > m$) Taylor series expanded about a^* , denoted as $T_{N,a^*}(a)$. To compute the remainder, the $(m+1)^{\text{st}}$ derivative of $T_{N,a^*}(a)$ is needed. Let $l = N - m - 1$. Then the $(m+1)^{\text{st}}$ derivative is the l^{th} order polynomial

$$T_{N,a^*}^{(m+1)}(a) = c_l(a - a^*)^l + c_{l-1}(a - a^*)^{l-1} + \dots + c_0 \quad (\text{B1})$$

and the remainder is given by

$$R_{m,a^*}(a) = \frac{1}{m!} \int_{a^*}^a [c_l(u - a^*)^l + c_{l-1}(u - a^*)^{l-1} + \dots + c_0] (a - u)^m du \quad (\text{B2})$$

Each term in the integral has the general form

$$I = \int_{a^*}^a (u - a^*)^l (a - u)^m du \quad (B3)$$

Let $u = \xi + a^*$. Then Eq. (B3) becomes

$$I_l = \int_0^{a-a^*} \xi^l [(a - a^*) - \xi]^m d\xi \quad (B4)$$

From entry 8 on page 68 in [9], we have the integral

$$\int x^l (a + bx^k)^m dx = \frac{b^m}{k} \sum_{i=0}^m \frac{(-1)^i m! J! \left(x^k + \frac{a}{b}\right)^{m-i} x^{k(J+i+1)}}{(m-i)! (J+i+1)!}, \quad J = \frac{l+1}{k} - 1 \quad (B5)$$

Comparing Eqs. (B4) and (B5) results in the following correspondences: $a = (a - a^*)$, $b = -1$, $k = 1$ and $x = \xi$. Then

$$I_l(\xi) = (-1)^m \sum_{i=0}^m \frac{(-1)^i m! l! [\xi - (a - a^*)]^{m-i} \xi^{l+i+1}}{(m-i)! (l+i+1)!} \quad (B6)$$

From this expression, the remainder is given in closed form as

$$R_{m,a^*}(a) = \frac{(-1)^m}{m!} [c_l I_l(\xi)|_0^{a-a^*} + c_{l-1} I_{l-1}(\xi)|_0^{a-a^*} + \dots + c_0 I_0(\xi)|_0^{a-a^*}] \quad (B7)$$